

Mapping the Pliocene Clay Deposits Using Remote Sensing and its Impact on the Urbanization Developments in Egypt: Case Study, East Sohag Area

Ahmed Mohamed Youssef

Received: 6 June 2007 / Accepted: 13 March 2008 / Published online: 1 April 2008
© Springer Science+Business Media B.V. 2008

Abstract In the current study, Thematic Mapper image was compiled along with field and laboratory investigation results to map the Pliocene clay deposits. These deposits have high swelling potential; consequently they will have a negative impact on the urbanization expansion surrounding the flood plain zone (Low desert zone) in Egypt. Principle Component and Minimum Noise Fraction techniques with the help of supervised classification were successful in the mapping of these deposits. The interpretation shows that the Pliocene clay deposits occupy most of the wadis terraces and part of the wadis floors, and sometimes they covered by Quaternary deposits (1–5 m of sand and gravel). The physio-chemical characteristics of these deposits indicate that the Pliocene clay ranges from silty clay to clay with small amounts of sand. Laboratory analysis (Atterberg limits, saturation degree, and cation exchange capacity) indicate the swelling characteristics of the Pliocene clay. Different classification systems were applied and all reveal the expansive nature of this soil, which should be taken into account for future development in the area.

Keywords Remote sensing · Geotechnical assessment · Mapping · Pliocene clay · Swelling

1 Introduction

Egypt has a rapidly growing population, now exceeding 70 million, concentrated in less than 5% of its land area. Like other areas, Egypt faces the demand for new urban communities to support its increasing population. The low desert zones, located between the Nile flood plain and the Limestone plateau, are the more desired areas for these activities. Most of these areas are occupied by marine Pliocene clay deposits.

Clay deposits are a major geologic hazard and cause extensive damage world-wide every year. They pose serious problems to engineering structures such as pipelines (Azam 2006); roadways and highways (rutting) (Aiban et al. 1998) especially in areas of rapid urban growth. Expansive soils owe their characteristics to the presence of swelling clay minerals. When wetted, the clay minerals absorb water molecules and expand. Conversely, when clay dries shrink, it leaves large voids in the soil. Swelling clays can control the behavior of virtually any type of soil if the clay is more than about 5% by weight. Soils with smectite clay minerals (montmorillonite) exhibit the most profound swelling properties. Generally, the swelling is restricted to soils containing clay minerals, which are susceptible to uptake water molecules in their chemical structure (Carter and Bentley 1991).

Different methods have been developed over the last few years to establishing faster and less expensive ways of estimating the swelling potential of engineering soils. Such methods have mainly consisted of

A. M. Youssef (✉)
Department of Geology, Sohag University, P.O. 82524,
Sohag, Egypt
e-mail: amyoussef70@yahoo.com

laborious and expensive laboratory tests. However, new methods for identification of these deposits from remote sensing as well as simple field and laboratory observations have recently been the subject of research. Chabrilat et al. (2002) found it possible to distinguish between the spectral response of three indicator clay minerals i.e., smectite, illite, and kaolinite based on airborne sensor data. However, access to such high-resolution data is still limited and study on the applicability of multispectral systems is still underway. On the other hand, the Landsat Thematic Mapper (TM) has provided extensive mapping capabilities (Goetz and Rowan 1981) and successes in the estimation of soil constituents such as organic matter (Ishida and Ando 1999), surface geologic materials (Bittick et al. 1994) and stages of iron and clay weathering (Riaza et al. 2000). With improving spectral resolution of spaceborne hyper-spectral sensors such as the ASTER (Advanced Spaceborne Thermal Emission and Reflection Radiometer), the capacity to resolve small spectral features from remote sensing in the future for such soil property mapping is becoming a reality.

Current engineering practice for characterization of these clay deposits involves time-consuming and expensive standard engineering tests. However, there are many simple and easy to use tests that will give good results for determination of the possible swelling hazards. Gill and Reaves (1957) described cation exchangeable capacity (CEC), saturation paste (SP), and plasticity index (PI) as some of the most representative properties in the estimation of swelling potential. Snethen et al. (1977) evaluated seventeen swelling indices and concluded that liquid limit (LL) and plastic index (PI) are the best indicators of potential swell, while Parker et al. (1977) established a swell index, and Lambe (1960) indicated that the plasticity index is superior to other indices. Schafer and Singer (1976) concluded that clay type rather than the clay content is more important and Thomas et al. (2000) described smectite content as critical in determining the swelling potential level. Karathanasis and Hajek (1985), in a study of montmorillonitic soils, found smectite content as the only consistent soil property that significantly correlated with laboratory measured shrink-swell potential.

The present study was undertaken to assess mapping and determining the expansive nature of Pliocene clay in East of Sohag Governorate, Egypt,

using remote sensing data (TM), field, and selected physicochemical and mineralogical soil properties. Different types of enhanced images are prepared using remote sensing and verified using field study.

2 Study Area

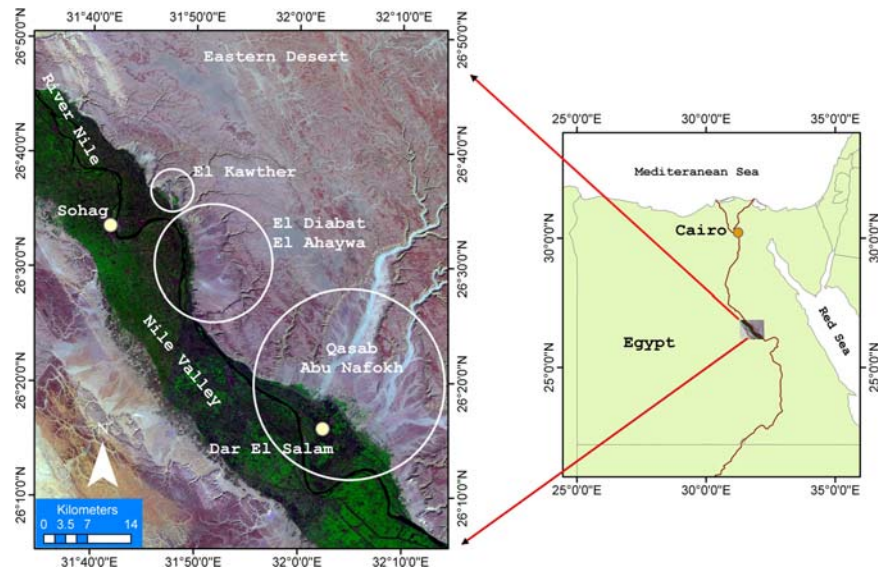
The study area is located east of Sohag Governorate, Egypt, midway between Cairo and Aswan in the low desert zone. It is situated between latitudes $26^{\circ}10'00''$ to $26^{\circ}45'00''$ N and longitudes $31^{\circ}40'00''$ to $32^{\circ}10'00''$ E (Fig. 1). The flood plain of the Nile Valley is completely utilized, and the population density is remarkably high; therefore finding new areas for development is an urgent issue. The desert areas between the old floodplain and the Eocene limestone plateau are the most promising areas for such development. The Egyptian government gives a very high priority to promoting and fostering economic development of territories outside the Nile valley. Due to the expected construction problems for the foundation of structures, sewage, road construction etc, because of the swell/shrink properties of these soils, there is urgency in finding a new and fast way to map and determine the distribution of these clay deposits. Figure (2) shows the distribution and damage of some buildings in the area due to Pliocene clays. Special provisions need to be taken to prevent these hazards in such constructions and other similar areas, making the current study even the more important. There are three areas that have been chosen for the Remote sensing applications as well as field and laboratory investigations including El-Kawther, El-Diabat to El-Ahaywa, and Qasab-Abu Nafokh (Fig. 1).

3 Material and Methods

3.1 Using Remote Sensing

Landsat 7 (Thematic Mapper TM) imagery acquired in 1984 has been used in the current study. The satellite data were enhanced to facilitate the delineation and interpretation of different thematic information using ENVI 4.3. The six none thermal bands (b1, b2, b3, b4, b5, and b7) with resolution of 30 m were used to prepare a layer stack map. Several data enhancement techniques were applied in the analysis, with both

Fig. 1 Location map of the study area



Univariate and Multivariate statistics used to reduce redundancies in the data for all the visible and infrared bands. Minimum Noise Fraction (MNF) and Principal Component Analysis (PCA) were the enhanced methods used in the current study. Finally, supervised classification was applied for these techniques to test their effectiveness.

Minimum Noise Fraction (MNF) is used to determine the inherent dimensionality of image data especially in hyperspectral data, to segregate noise in the data, and to reduce the computational requirements for subsequent processing (Boardman and Kruse 1994). The MNF transform is essentially two cascaded principal component transformations (Green et al. 1988) where the first transformation based on an estimated noise covariance matrix decorrelates and scales the noise in the data. This first step results in band-to-band correlations. The second step is a standard Principal Component transformation of the noise-whitened data. For further spectral processing, the inherent dimensionality of the data is determined by examination of the final eigen values and the associated images. The data can be divided into two parts: one part associated with large eigen values and coherent eigen images, and a complimentary part with near unity eigen values and noise dominated images. By using only the coherent portions, the noise is separated from the data, thus improving the spectral processing results.

In Principal Component Analysis (PCA), one can use either standard or selective analysis, the difference

being that in the former all bands will be used, while in the later, only certain bands are chosen (Crosta and Moore 1989). The later is otherwise known as the Crosta technique or Feature Oriented Principal Components Selection (FPCS) whose analysis of eigenvector values allows identification of the principal components that contain spectral information about specific materials, as well as the contribution of individual original bands in relation to the spectral response of the materials of interest. This technique indicates whether the materials are represented by bright or dark pixels based on the sign and magnitude of the eigenvectors.

Both the images that derived from PCA and MNF techniques have been subjected to the supervised classification to extract the areas that Pliocene clay is detected.

3.2 Field and Laboratory Analysis

A reconnaissance survey was conducted in the investigated area in order to gain an appreciation of the broad soil patterns. GPS Navman (± 5 m horizontal resolution) was used in the field to accurately locate soil sampling and mobile GIS was used to accurate map of these units. Twenty-eight soil samples were collected from the Pliocene clay deposits (six samples are collected from the surface and 22 were collected from subsurface). The soil samples were analyzed in the laboratory to determine mineralogical composition from X-ray diffraction (XRD)

Fig. 2 Field photographs from the study area (a) Photograph showing the Pliocene clay in Construction area; (b) photograph showing the distribution of Pliocene clay in new planning area; (c) photograph showing cracks due to Pliocene clay under a building; and (d and e) photographs showing Pliocene clay distribution (~ 0.5 m) under urban areas



analyses and swelling potential using standard engineering tests. Samples were first air dried, grounded, and sieved to remove coarse fragments >2 mm. Laboratory analyses including particle-size distribution, cation exchange capacity, atterberg limits, and clay mineralogy have been conducted. Table (1) shows the different laboratory analysis of this study.

4 Results

4.1 Using Remote Sensing

Univariate analysis are shown in Table (2), the results show band 4 has the smallest variance due to its low contrast and band 5 has the largest variance

Table 1 Soil analysis for Pliocene clay including soil property, methods, and reference

| | Soil property | Method | Reference |
|---|-----------------------------------|--|------------------------|
| 1 | Visual inspections | Free swell | Holtz and Gibbs (1956) |
| 2 | Particle size distribution (PSD) | Sieve and pipette method | Gee and Bauder (1986) |
| 3 | Aterberge limites (LL, PL, PI) | ASTM method D4318 | ASTM (1993) |
| 4 | Cation exchangable capacity (CEC) | NH ₄ OAc, pH 7 and BaCl ₂ -TEA, pH 8.2 | Thomas (1982) |
| 5 | Saturation paste (SP) | Saturation and oven drying at 105° | |
| 6 | X-ray diffraction (XRD) | | Jackson (1975) |

Table 2 Univariate analysis on the six bands of the Thematic Mapper image

| | Min | Max | Mean | S.D. | Variance |
|--------|-----|-----|--------|-------|----------|
| Band 1 | 86 | 254 | 159.27 | 34.02 | 1157.36 |
| Band 2 | 32 | 169 | 88.43 | 25.83 | 667.18 |
| Band 3 | 29 | 254 | 127.19 | 46.6 | 2171.56 |
| Band 4 | 14 | 218 | 118.09 | 24.31 | 590.97 |
| Band 5 | 11 | 254 | 200.44 | 69.53 | 4834.42 |
| Band 7 | 3 | 236 | 115.74 | 48.23 | 2326.13 |

Table 3 Correlation matrix of the six Thematic Mapper bands

| | Band 1 | Band 2 | Band 3 | Band 4 | Band 5 | Band 7 |
|--------|--------|--------|--------|--------|--------|--------|
| Band 1 | 1 | 0.99 | 0.98 | 0.83 | 0.94 | 0.95 |
| Band 2 | 0.99 | 1 | 0.99 | 0.85 | 0.95 | 0.96 |
| Band 3 | 0.98 | 0.99 | 1 | 0.83 | 0.96 | 0.97 |
| Band 4 | 0.83 | 0.85 | 0.83 | 1 | 0.8 | 0.79 |
| Band 5 | 0.94 | 0.95 | 0.96 | 0.80 | 1 | 0.98 |
| Band 7 | 0.95 | 0.96 | 0.97 | 0.79 | 0.98 | 1 |

Table 4 Statistics of the Minimum Noise Fraction transformation images

| | Min | Max | S.D. | Eigen value |
|--------|-------|------|------|-------------|
| Band 1 | −14.0 | 29.2 | 11.9 | 143.7 |
| Band 2 | −21.1 | 51.6 | 4.2 | 17.9 |
| Band 3 | −17.7 | 21.3 | 3.2 | 10.5 |
| Band 4 | −13.8 | 30.7 | 2.6 | 7.0 |
| Band 5 | −17.3 | 38.9 | 2.1 | 4.5 |
| Band 7 | −15.9 | 10.1 | 1.3 | 1.7 |

due to the large differences in the spectral response of the various materials contained in the image. The correlation matrix (Table 3) represents the multivariate statistics and indicates that bands 1, 2, 3, 5, and 7 are highly correlated, and therefore their information is redundant. The lowest correlation is obtained for bands 4 making it the most important in establishing differences on the basis of spectral information.

Table 4 gives summarized statistics of the MNF transformation. From the statistics it is obvious that the first three bands, with large eigen values would be the most useful to represent the spectral information, contained in the images. The first MNF

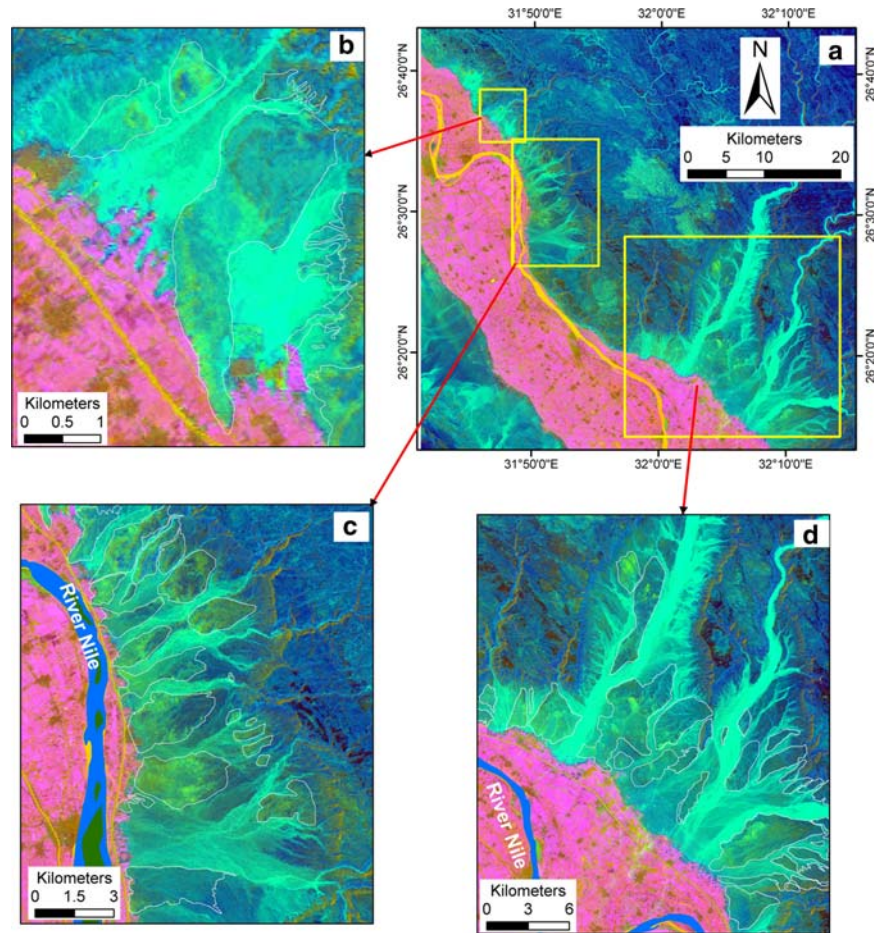
image consisted of the highest variance and was interpreted to represent variation in the study area among the surface materials. The second MNF had strong negative loading from band 5 and thus was assigned to information on bare soil. The third MNF image gave a strong negative loading from band 4 and was assigned to vegetation. Other MNF images were found to consist of noise and thus were not considered in the proceeding analysis. Figure (3) shows the combination of MNF 1, 2, 3 in RGB, they are clearly marking out the areas of Pliocene clay with a bright green color. Figure (4) shows the supervised classification for the MNF image in which the Pliocene clay areas appear in red color and the surrounding materials in black.

For the principal component transformation, six of the seven TM bands (1, 2, 3, 4, 5, and 7) are shown in Table 5. The first three principal components (PC1, 2, 3) were assumed to consist of information on the study area. A map composite of PC 1, 2, 3 in RGB, respectively was thought to map the Pliocene clay as bright blue color (Fig. 5). On the other hand, Fig. 6 shows the supervised classification for the PCA image in which the Pliocene clay areas appear in red color and the surrounding materials in black.

4.2 Field and Laboratory Analysis

From the visual inspections of the most analysis and clay deposits in the field, it was noticed that the color of the Pliocene clay deposits range from greenish grey to dark brown (chocolate clay). Moreover, the soils in the field are typically desiccated as soon as they are exposed to the sun, with smooth sliding surfaces. One of the more simple procedures, the free swell test (Holtz and Gibbs 1956), was applied. The free swell is determined by comparing the initial volume with the final volume of the clay sample. Generally, soils having free swell values greater than 100% are considered hazardous, while soils with free swell values below 50% probably do not exhibit appreciable volume changes. However, Dawson (1953) reported that several Texas clays with free swell values of about 50% showed extensive expansion. The free swell analysis of Pliocene clay ranges from 69.7 to 74.1% with an average of 71.5% which indicates expansive characteristics. In the field, expansive clay soils can be easily recognized in the dry season by the deep cracks in roughly polygonal patterns. The value

Fig. 3 Color composite of the Minimum Noise Fraction 1, 2, and 3 in RGB respectively for the study area in which the Pliocene clay appear in light green (a) image showing the whole area; (b) image showing El- Kawther area; (c) image showing El-Diabat–El-Ahaywa area; and (d) image showing Qasab–Abu Nafokh area. The field mapping is shown in black lines in images b, c, and d



ranges of different tests are shown in Table 6 and they will be discussed in the following parts.

Other types of tests done in the laboratory included plasticity characteristics and volume change behavior, which are directly related to the amount of colloidal particles ($<1 \mu\text{m}$) in soils (Anderson et al. 1973; Nelson and Miller 1992). The Particle Size Distribution (PSD) of the obtained samples was analyzed by sieving and sedimentation (Gee and Bauder 1986; Head 1992). The results indicate that the soil is composed of 30–72% clay, 55–25% silt, and 3–15% sand.

Atterberg limits (liquid limit, plastic limit, and plasticity index) were measured using Casagrande's liquid device (ASTM method D4318) (American Society for Testing and Materials 1993). The properties of plastic clays are a function of the electrochemical behavior of the clay minerals (Carter and Bentley 1991). The results show that the liquid

limit ranges from 44 to 62% and the plastic limit from 25.9 to 37.5%. The plastic index for the Pliocene clay samples ranges from 13.5 to 36.1%.

The cation exchange capacity (CEC) is used to estimate the shrink-swell potential, in addition to other engineering properties of a soil. Cation exchange capacity is the quantity of exchangeable cations needed to balance the negative charge on the surface of clay particles and is usually expressed in milli-equivalents per 100 g (meq/100 g) of dry clay. A method proposed by Thomas (1982) was used to determine CEC in this study. CEC is related to the amount and type of clay present in a soil. As clay content and swelling clays increase in a soil, the CEC and shrink-swell potential also increases. High CEC values indicate a high surface activity. The results of 28 samples collected from the Pliocene clay in the study area show that the CEC ranges from 27 to 128 meq/100 g. On the other hand, the Cation exchange activity CEAc was determined

Fig. 4 Supervised classification applied on the Minimum Noise Fraction image (a) the Minimum Noise Fraction for the study area; (b) image showing El- Kawther area; (c) image showing El-Diabat–El-Ahaywa area; and (d) image showing Qasab–Abu Nafokh area. The Pliocene clay appears in red where the unclassified areas appear in black. Field mapping is shown in white lines for images b, c, and d.

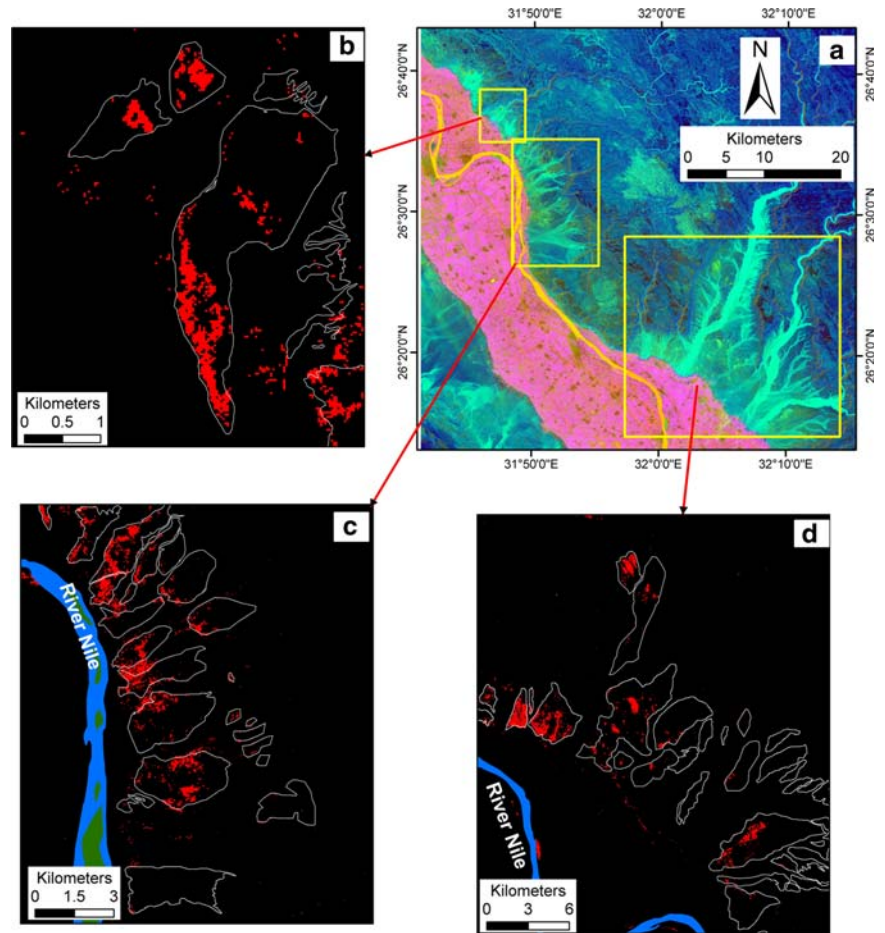


Table 5 Principal component analysis of the study area

| | Band 1 | Band 2 | Band 3 | Band 4 | Band 5 | Band 7 | Eigen value (%) |
|------|--------|--------|--------|--------|--------|--------|-----------------|
| PC 1 | 0.31 | 0.23 | 0.43 | 0.19 | 0.64 | 0.45 | 96.38 |
| PC 2 | 0.0.31 | 0.25 | 0.31 | 0.66 | −0.49 | −0.23 | 2.01 |
| PC 3 | 0.0.35 | 0.22 | 0.4 | −0.70 | −0.38 | 0.10 | 1.2 |
| PC 4 | 0.0.51 | 0.0.6 | −0.18 | −0.14 | 0.39 | −0.72 | 0.25 |
| PC 5 | 0.0.59 | −0.09 | −0.62 | 0.08 | −0.17 | 0.45 | 0.1 |
| PC 7 | 0.23 | −0.90 | 0.35 | 0.04 | −0.02 | −0.01 | 0.01 |

according to the following equation obtained from Pearring (1963) and Holt (1969).

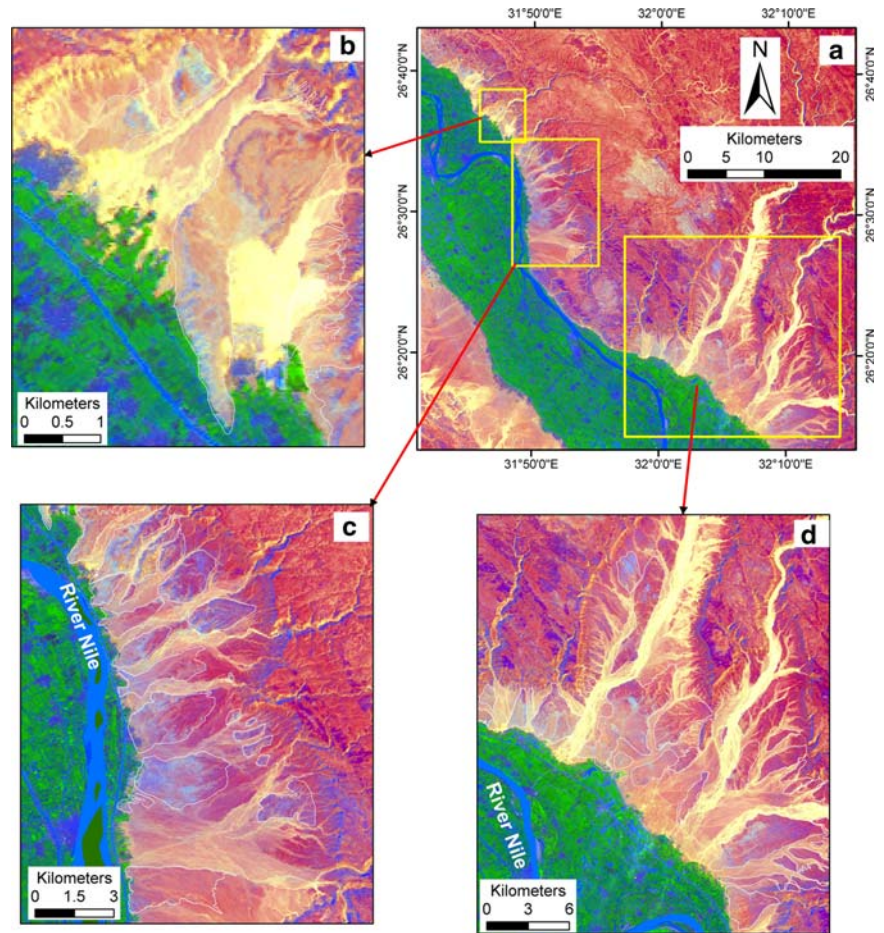
$$CEA_c = CEC / \text{clay content}$$

The results of CEA_c show that the values are ranging from 0.8 to 1.15.

For the X-ray diffraction analysis, part of the clay sample is separated after being pretreated according

to the procedure described by Jackson (1975). The clay samples are X-rayed after being Ca-saturated at 25°C, Ca-saturated and glycolated, and K-saturated at 25°C. Identification of the clay minerals was carried out following the guidelines provided by Black (1965), MacEwan (1980), Carroll (1970), and Weed (1977). The results are given in Table 7 and Fig. 7.

Fig. 5 Color composite of the Principle Component Analysis 1, 2, and 3 in RGB respectively for the study area in which the Pliocene clay appear in light blue (a) image showing the whole area; (b) image showing El-Kawther area; (c) image showing El-Diabat–El-Ahaywa area; and (d) image showing Qasab–Abu Nafokh area. The field mapping is shown in white lines for images b, c, and d.



5 Discussion

The uses of Landsat TM images for soil mapping has always been hindered by vegetation cover (Ruiz-armenta and Prol-ledesma 1998) and complex methods are required to remove the vegetation influence. However, in this study we use Landsat image of 1984 at which time there was limited development in the area. The results of this study demonstrate different methods can be used for mapping the Pliocene clay. Improvements on these separations were made by the application of different statistical analysis methods to decorrelate the image bands and enhance the spectral response. The higher order principal components retained most spectral features typical of clay minerals i.e. the anomalous high reflectance and absorption of band 5 and 7 respectively that are distinctive of hydroxide bearing minerals and was evident in the bare soil areas. This confirms the phenomenon as

important for swelling soils mapping from remote sensing imagery, thus providing another use of spaceborne sensors in the identification and mapping of soil physical properties. The results show the potential application of TM data by using PCA and MNF techniques with the help of supervised classification method in mapping the Pliocene clay based on spectral and spatial analysis.

The remotely sensed results were verified by field mapping using GPS. However, the spatial agreement of the produced maps with real field maps shows validated in a few spots by checking (Figs. 4 and 6). This represents a short as a validating tool in terms of surface distribution of the Pliocene clays related to field mapping. The reason for that is because in some areas the Pliocene clay deposits are covered by gravel and sand deposits with a thickness ranges from 1 to 5 m. These gravel and sand deposits hide the detection of these clay deposits by using remote sensing data.

Fig. 6 Supervised classification applied on the Principle Component Analysis image (a) the Principle Component Analysis for the study area; (b) image showing El-Kawther area; (c) image showing El-Diabat–El-Ahaywa area; and (d) image showing Qasab–Abu Nafokh area. The Pliocene clay appears in red where the unclassified areas appear in black. Field mapping is shown in white lines for images b, c, and d.

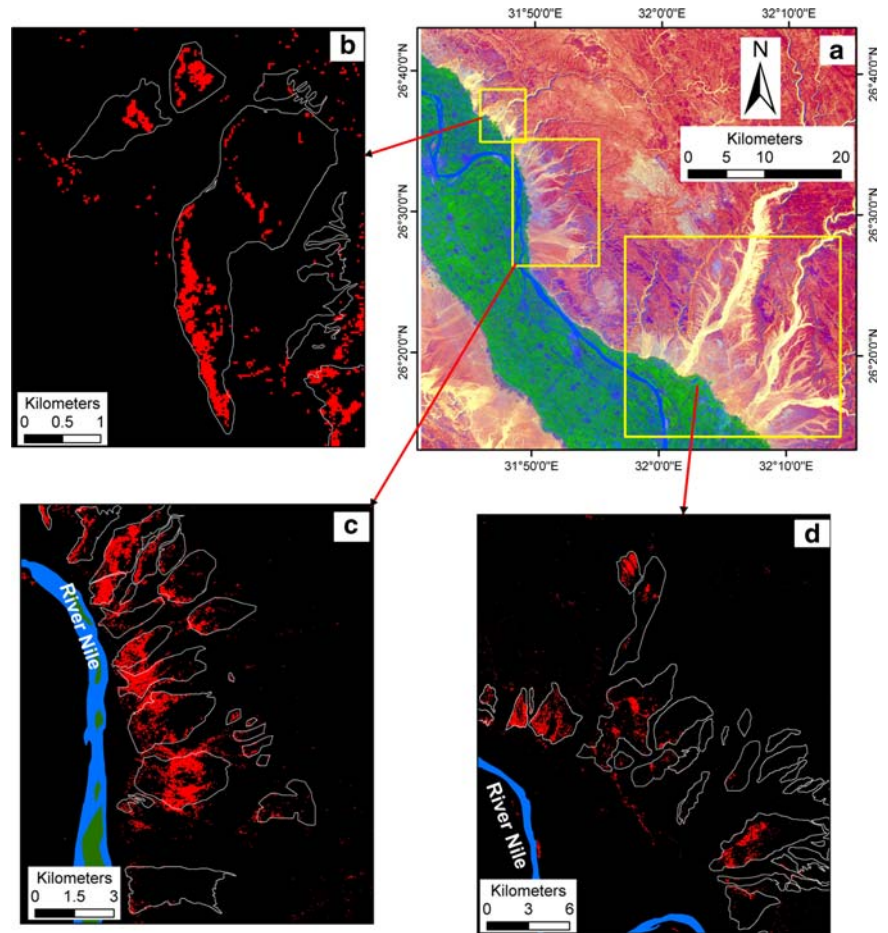


Table 6 Physio-chemical and engineering characteristics of the Pliocene clay in the study area

| Property | Minimum | Maximum | Average |
|--------------|---------|---------|---------|
| SP % | 53.5 | 72.7 | 63.6 |
| CEC | 26.71 | 128 | 54.77 |
| LL % | 44 | 62 | 50.05 |
| PL % | 25.9 | 37.5 | 30.73 |
| PI % | 13.5 | 36.1 | 22.33 |
| Clay% | 30 | 72 | 52.75 |
| Free swell % | 69.7 | 74.14 | 71.47 |
| AC | 0.409 | 0.722 | 0.501 |
| CEAc | 0.8 | 1.15 | 1.05 |
| SPP | 1.35 | 1.62 | 1.47 |

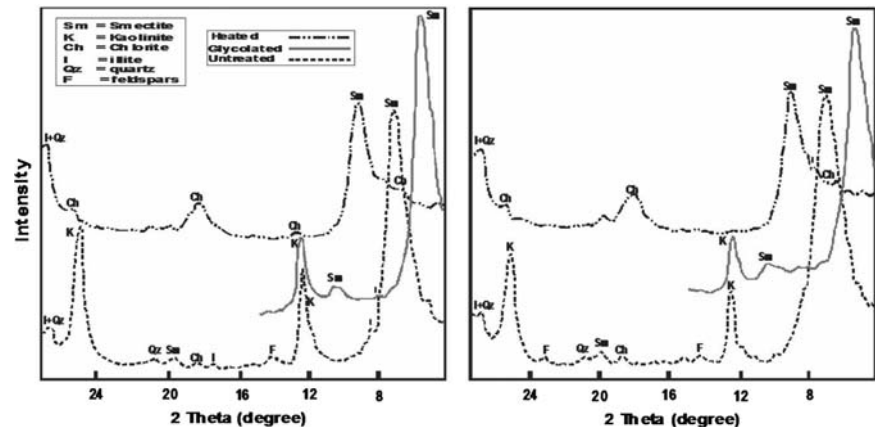
However, the results show that there is a good agreement of using remote sensing data to map the Pliocene clay deposits appeared on surface.

Achieving a satisfactory classification of expansive soils requires knowledge of the geotechnical parameters that characterize swelling. The literature contains a considerable number of empirical techniques for assessing the swelling potential of soils. Some authors consider that this potential can be linked to a single parameter (Sneath 1980). Other authors think that at least three parameters are necessary in order to evaluate the swelling potential of soils such as Holtz and Gibbs (1956). Swell indicators are soil properties, such as clay content, clay type, and the various physicochemical properties that directly or indirectly contribute to swelling tendencies. Swell potential refers to the definition of low, moderate, high, and very high classes according to different authors.

The classification quoted by Chen (1988), defines the swelling potential as a function of the liquid limit as follows: Low when $LL = 20\text{--}35$, moderate when a

Table 7 The calculated peak height and peak area of the different clay minerals

| Sample No. | Peak height (%) | | | | Peak area (%) | | | |
|------------|-----------------|-----------|----------|--------|---------------|-----------|----------|--------|
| | Smectite | Kaolinite | Chlorite | Illite | Smectite | Kaolinite | Chlorite | Illite |
| 7 | 88.5 | 9.3 | 1 | 1.2 | 74.8 | 21.7 | 2.8 | 0.8 |
| 25 | 79.8 | 18 | 1.5 | 0.8 | 61.1 | 34.7 | 2.9 | 1.2 |

Fig. 7 Shows X-ray diffraction for two Pliocene clay samples

LL = 35–50, and high when LL = 50–70. The liquid limit of the Pliocene clay ranges from 44 to 62, and, hence, indicates that the swelling potential for the soil is ranging between moderate and high. Seed et al. (1962) proposed a classification which relates the swelling potential (SP) to the plasticity index. The swelling potential is defined as the percentage swelling of a clay sample that has been compacted to the optimum proctor water content and subjected to a load of 7 kPa. It can be correlated to the PI by following the empirical relationship:

$$SP = 1.10^{(-5)}PI^{(2.24)}$$

This classification is as follows: low when PI = 0–10 or SP% = 0–1.5, moderate when PI = 10–20 or SP = 1.5–5, and high when PI = 20–35 or SP% = 5–25. The plasticity index of the Pliocene clay ranges from 13.5 to 36.1, so that the swelling potential for the Pliocene clay is between moderate to very high.

Based on Holt (1969), Parker (1977), and Hamberg (1985), various classification methods have been proposed over the years by different researchers. The swelling potential is considered to be a function of the saturation paste and mineralogy, and the classification is as follows: low when SP <30 which

indicates that kaolinite >50%, moderate when SP = 30–45 which indicates that illite >25%, and high if SP >45 which indicates that smectite >50%. The saturation paste of the Pliocene clay of the study area ranges from 53.5 to 72.7, which indicates a high swelling potential. This also complies that the smectite mineral constitutes more than 50% of the clay fraction, which is considered by the XRD analysis that indicated a dominant of smectite in the clay deposits.

Skempton (1953), Peering (1963), and Holt (1969) proposed a method of using clay content to normalize the plastic index and CEC to obtain Activity (Ac) and cation exchange activity (CEAc) respectively. A classification technique has been established by McKen and Hamberg (1981) and Hamberg (1985), and modified to include the clay mineral type by Nelson and Miler (1992) to classify soils into swelling potential groups and dominated clay mineral type. The soils are classified into three swelling potential classes based on classification criteria as shown in Table 8. The criteria are a result of normalizing measured properties with the clay content giving a relative measure of the clay influence on the various properties.

The results of the Pliocene clay indicate that the activity is ranging from 0.41 to 0.72 which indicates moderate to high swelling potential; the cation

Table 8 Normalized physiochemical parameters and modified clay mineral type allocation (after Nelson and Miller 1992)

| Activity (Ac) | Cation activity (CEA _C) | NSP | Swelling potential | Clay mineral |
|---------------|-------------------------------------|-------|--------------------|----------------|
| >0.6 | >0.5 | >1.5 | High | Smectite >50% |
| 0.4–0.6 | 0.4–0.5 | 1–1.5 | Moderate | Illite >25% |
| <0.4 | <0.4 | <1 | Low | Kaolinite >50% |

activity ranges between 0.8 and 1.15 which indicates that the clay has a high swelling potential, and the normalized saturation paste (NSP) ranges between 1.35 and 1.62, indicating that the clay has a moderate to high swelling potential.

Another method to evaluate the hazard degree of Pliocene clay uses a swelling potential rating system, consisting of three stages according to different levels of risk. The third index can be used as a fast reconnaissance field index and the first as a detailed site characterization where the preliminary results show the need for a follow up. The three levels are summarized in Table 5 and the following equations (Table 9).

$$\text{Level 1} = \text{Ac} + \text{CEAc} + \text{NSP} + \text{LEP}$$

$$\text{Level 2} = \text{Ac} + \text{CEAc} + \text{NSP}$$

$$\text{Level 3} = \text{NSP}$$

According to this classification level 2 and 3 can be used for the evaluation of Pliocene clay. Level 3 shows that the SSP is ranging from 1.35 to 1.62 which indicates that the Pliocene clay has a high rating of swelling potential. For level 2 the sum of these parameters are in range of 2.97–3.18, which more than 2.6, and indicates that the Pliocene clay has a high rating of swelling potential.

Several, treatment procedures are available for stabilizing expansive soils (Nelson and Miller 1992). Removal of expansive soil and replacement with a non-expansive material is a common method of reducing shrink-swell risk. If the expansive soil or stratum is thin, then the entire layer can be removed. However, frequently the soil or stratum extends to a

depth too great to remove economically. Pre-wetting a site to increase the moisture content can eliminate an expansive soil problem if the high moisture content can be maintained. Soils with low hydraulic conductivity may take years to pre-wet and conversely soils with high hydraulic conductivity may never sufficiently wet. Lime stabilization has been used extensively in highway projects. The addition of lime creates several stabilizing reactions. The solubility of silica is increased in a higher pH environment and silica becomes available as a cementing agent. The lime also provides a divalent cation that can form Casilicates and Ca–Al hydrates that increase soil strength. The presence of organics, sulfates, and some iron compounds can inhibit lime stabilization reactions. Fly ash (product of coal combustion) has also been used instead of lime as a stabilizing agent; the reduction is attributed to bonding of soil particles to the fly ash resulting in flocculation (Ferguson 1993).

6 Conclusion

Expansive soils cause billions of dollars of damage to homes and property all over the world each year. Damage can be avoided or mitigated if the soil shrink and swell properties are known before construction. Predicting shrink-swell potential accurately requires both the knowledge of which soil properties influence shrinking and swelling and the magnitude of these parameters. In the study different types of techniques were used to evaluate the Pliocene clay characteristics and distributions in the area. The techniques include: (1) remote sensing and GIS to delineate the distribution of the Pliocene clay deposits; (2) field reconnaissance using mobile GIS to collect sample locations, as well as field mapping and verification; and (3) laboratory analysis to determine the physiochemical characteristics to estimate the swelling potential.

This study has established that using different image enhanced techniques such as MNF and PCA

Table 9 The classification based on the swelling potential rating system

| Level 1 | Level 2 | Level 3 | Rating | Mineralogy |
|-----------|---------|---------|----------|--------------------|
| >2.69 | >2.6 | >1.0 | High | Smectite |
| 1.75–2.69 | 1.7–2.6 | 0.5–1.0 | Moderate | Illite mixed layer |
| <1.75 | <1.7 | <0.5 | Low | Kaolinite |

with the help of supervised classification were useful in establishing differences between different deposits and detect the Pliocene clay deposits. The remote sensed data was improved further by using of the field and laboratory verification. This was concluded to show the imagery potential in characterizing the soils physicochemical properties, thus providing a tool for establishing the soil properties at a wider scale.

The laboratory analysis indicates that the Pliocene clay in the study area has expansive characteristics. The physicochemical characteristics were used to detect the clay behavior included Atterberg limits, XRD, grain size distribution, saturation paste, free swelling, and visual inspection.

Also, several indices were employed for classification, as liquid limit, plastic limit, plasticity index, CEC, cation activities, clay contents, XRD, activities, saturation paste, and free swelling. All classification methods indicate that the Pliocene clay has a moderate to high swelling potential. The most trustworthy method, i.e., the expansive soil rating system to assess shrink-swell potential, also indicates that the Pliocene clay has a moderate to high swelling potential. These findings should be taken into account for future development in the Sohag region, Egypt.

References

- Aiban SA, Al-Abdul Wahhab HI, Al-Amoudi OSB, Ahmed HR (1998) Performance of a stabilized marl base: a case study. *Construct Build Mater* 12(6–7):329–340
- American Society for Testing Materials (1993) Annual book of ASTM standards. Construction. Section 4. Soil and rock; dimension stone; geosynthesis, vol 04.08. ASTM, Philadelphia
- Anderson JU, Kamal EF, O'Connor GA (1973) Factors affecting the coefficient of linear extensibility in vertisols. *Soil Sci Soc Am Proc* 37:298–299
- Azam S (2006) Large-scale odometer for assessing swelling and consolidation behaviour of Al-Qatif clay. In: Al-Rawas AA, Goosen MFA (eds) *Expansive soils: recent advances in characterization and treatment*. Balkema Publishers-Taylor and Francis, The Netherlands, pp 85–99
- Bittick SM, Morgan KM, Busbey AB (1994) Preliminary spectral analysis of calibrated reflectance patterns to map the distribution of alluvial fans on the Rosillos laccolith in Brewster County, Texas. *Proceeding 10th thematic conference on geologic remote sensing, San Antonio, Texas, 9–12 May (Ann, Arbor, MI: ERIM)*, pp 151–157
- Black CA (1965) *Methods of soil analyses Part 1. Physical and mineralogical properties*. American Society Agronomy, Inc. Pub, Madison, USA
- Boardman JW, Kruse FA (1994) Automated spectral analysis: a geological example using AVIRIS data, northern Grapevine Mountains, Nevada. *Proceeding 10th thematic conference on geologic remote sensing, San Antonio, Texas, 9–12 May*, pp 407–418
- Carroll D (1970) *Clay minerals: a guide to their X-ray identification*. Geol Soc of America Special Paper 128. Geological Society of America, Boulder, Colorado
- Carter M, Bentley SP (1991) *Correlations of soil properties*. Pentech Press, London, UK
- Chabrilat S, Goetz AFH, Krosley L, Olsen HW (2002) Use of hyperspectral images in the identification and mapping of expansive clay soils and the role of spatial resolution. *Remote Sens Environ* 82:431–445
- Chen FH (1988) *Foundations on expansive soils*. Elsevier, USA
- Crosta AP, Moore JMcM (1989) Enhancement of Landsat Thematic Mapper imagery for residual soil mapping in SW Minas Gerais State, Brazil: a prospecting case history in Greenstone Belt terrain. *Proceedings of the Seventh Thematic Conference on Remote Sensing for Exploration Geology, Calgary, Alberta, Canada, 2–6 October*, pp 1173–1187
- Dawson RF (1953) Movement of small houses erected on an expansive clay soil. *Proc 3rd Intl Conf Soil Mech Found Eng* 1:346–350
- Ferguson G (1993) Use of self-cementing fly ashes as a soil stabilization agent. In Sharp KD (eds) *Fly ash for soil improvement*. p 1–14. Am Soc Civil Eng Geotech Pub 36
- Gee GW, Bauder JW (1986) Particle-size analysis. In: Klute A (ed) *Methods of soil analysis, Part 1, 2nd edn*. ASA and SSSA, Madison, pp 383–411 *Agron. Monogr.* 9
- Gill WR, Reaves CA (1957) Relationships of Atterberg limits and cation exchange capacity to some physical properties of soil. *Soil Sci Soc Am Proc* 21:491–494
- Goetz AFH, Rowan LC (1981) Geologic remote sensing. *Science* 211:781–791
- Green AA, Berman M, Switzer P, Craig MD (1988) A transformation for ordering multispectral data in terms of image quality with implications for noise removal. *IEEE Trans Geosci Remote Sens* 26(1):65–74
- Hamberg DJ (1985) A simplified method for predicting heave in expansive soils. M.S. thesis, Colorado State University, Fort Collins, CO, USA
- Head KH (1992) *Manual of soil laboratory testing, vol. I, Soil classification and compaction tests*. Pentech Press, London
- Holt JH (1969) A study of physico-chemical, mineralogical and engineering index properties of fine grained soils in relation to their expansive characteristics. Ph.D. Dissertation, Texas A&M Univ., College Station, TX
- Holtz WG, Gibbs HJ (1956) Engineering properties of expansive clays. *Trans ASCE* 121:641–677
- Ishida T, Ando H (1999) Use of disjunctive cokriging to estimate soil organic matter from Landsat Thematic Mapper image. *Int J Remote Sens* 20(8):1549–1565
- Jackson ML (1975) *Soil chemical analyses advanced course*. Pub. By author, Madison
- Karathanasis AD, Hajek BF (1985) Shrink-swell potential of montmorillonitic soils in udic moisture regimes. *Soil Sci Soc Am J* 49:159–166
- Lambe TW (1960) *The character and identification of expansive fed. Housing Admin. Rep. 701*. U.S. Gov. Print. Office, Washington, DC

- MacEwan DMC, Wilson MJ (1980) Interlayer and intercalation complexes of clay minerals. In: Brindley GW, Brown G (eds) Crystal structures of clay minerals and their X-ray identification, chapter 3. Monograph 5 of Mineralogical Society, London
- McKeen RG, Hamberg DJ (1981) Characterization of expansive soils. Transportation. Research. Record. 790, Transportation. Research Board, USA
- Nelson JD, Miller DJ (1992) Expansive soils: problem and practice in foundation and pavement engineering. John Wiley & Sons, New York
- Parker JC, Amos DF, Kaster DL (1977) An evaluation of several methods of estimating soil volume change. Soil Soc Am J 41:1059–1064
- Pearring JR (1963) A study of basic mineralogical, physical-chemical, and engineering index properties of laterite soils. Ph.D. Dissertation, Texas A&M Univ., College Station, TX, USA
- Riaza A, Mediavilla R, Santistieban JI (2000) Mapping geological stages of climate-dependent iron and clay weathering alteration on lithologically uniform sedimentary units using Thematic Mapper imagery (Tertiary Duero Basin, Spain). Int J Remote Sens 21(5):937–950
- Ruiz-Armenta JR, Prol-Ledesma RM (1998) Techniques for enhancing the spectral response of hydrothermal alteration minerals in Thematic Mapper images of Central Mexico. Int J Remote Sens 19(10):1981–2000
- Schafer WM, Singer MJ (1976) Influence of physical and mineralogical properties on swelling of soils in Yolo County, California. Soil Sci Soc Am J 40:557–562
- Seed HB, Woodward RJ Jr, Lundgren R (1962) Prediction of swelling potential for compacted clays. J Soil Mech Found Div Am Soc Civil Eng 88(SM3):53–87
- Skempton AW (1953) The colloidal activity of clay. In: Proceedings of the third international conference on soil mechanics and foundation engineering vol. I, London, pp 57–61
- Snethen DR (1980) Characterization of expansive soils using soil suction data 4th international conference on expansive soil, pp 54–75
- Snethen DR, Johnson LD, Patrick DM (1977) An evaluation of expedient methodology for identification of potentially expansive soils. Soil and Pavements Laboratory, U.S. Army Eng. Waterway Exp. Sta., Vicksburg, MS, Rep. No. FHWA-RE-77-94, NTIS PB-289-164
- Thomas GW (1982) Exchangeable cations. In: Page AL (ed) Methods of soil analysis, Part 2, 2nd edn. ASA and SSSA, Madison, pp 159–165, Agron Monogr 9
- Thomas PJ, Baker JC, Zelazny LW (2000) An expansive soil index for predicting shrink-swell potential. Soil Sci Soc Am J 64:268–274
- Weed SB (1977) Minerals in soil environment. Soil Sci Soc Am J 56:1640–1645